Estimating and correcting the amplitude radiation pattern of a virtual source

Joost van der Neut[1] and Andrey Bakulin[2]

ABSTRACT

In the virtual source (VS) method we crosscorrelate seismic recordings at two receivers to create a new data set as if one of these receivers were a virtual source and the other a receiver. We focus on the amplitudes and kinematics of VS data, generated by an array of active sources at the surface and recorded by an array of receivers in a borehole. The quality of the VS data depends on the radiation pattern of the virtual source, which in turn is controlled by the spatial aperture of the surface source distribution. Theory suggests that when the receivers are surrounded by multicomponent sources completely filling a closed surface, then the virtual source has an isotropic radiation pattern and VS data possess true amplitudes. In practical applications, limited source aperture and deployment of a single source type create an anisotropic radiation pattern of the virtual source, leading to distorted amplitudes. This pattern can be estimated by autocorrelating the spatial Fourier transform of the downgoing wavefield in the special case of a laterally invariant medium. The VS data can be improved by deconvolving the VS data with the estimated amplitude radiation pattern in the frequency-wavenumber domain. This operation alters the amplitude spectrum but not the phase of the data. We can also steer the virtual source by assigning it a new desired amplitude radiation pattern, given sufficient illumination exists in the desired directions. Alternatively, time-gating the downgoing wavefield before crosscorrelation, already common practice in implementing the VS method, can improve the radiation characteristics of a virtual source.

INTRODUCTION

The virtual source (VS) method is an innovative technique to image and monitor the subsurface in cases where a complex overburden prevents seismic techniques and vertical seismic profiling (VSP) to deliver good results (Bakulin and Calvert, 2004, 2006). Placing receivers below the complex overburden allows us to measure directly the propagation response and apply time-reversal logic to redatum surface shots into downhole receiver locations without the requirement of any additional information about the medium between sources and receivers. Redatumed shots are called virtual sources. Various applications of the virtual source method have been reported in the literature: imaging and monitoring below a complex overburden using horizontal wells with P-waves (Bakulin and Calvert, 2004, 2006) and S-waves (Bakulin and Calvert, 2005), salt-flank imaging using a vertical well (Hornby et al., 2006; Willis et al., 2006), velocity estimation from virtual check shots with P-waves (Mateeva et al., 2006) and S-waves (Bakulin et al., 2007b), look-ahead VSP imaging (Mateeva et al., 2007), redatuming of ocean-bottom seismic data (Mehta et al., 2007) and a variety of other uses (Bakulin et al., 2007c; Schuster and Zhou, 2006). Most authors focus on the kinematics of the retrieved signals: little has been said about the amplitudes of VS data. Characterization applications such as AVO are not reported with VS data although VS is advocated as a sensitive monitoring tool. Indeed, time-lapse imaging of VS data produces highly repeatable data even in the presence of a complex and changing overburden (Bakulin and Calvert, 2004; Bakulin et al., 2007c). However, quantitative interpretation of 4D signals requires confidence in the recovered VS amplitudes. If amplitude distortions vary significantly from location to location, then 4D anomalies will exhibit this spatial imprint and create a problem for interpretation.

The theory behind the virtual source method is closely related to seismic interferometry, with various applications ranging from ultrasonics (Weaver and Lobkis, 2002) to seismology (Campillo and Paul, 2003). In all cases, a Green's function between two receiver lo-

cations is retrieved by crosscorrelating seismic observations at these two receiver locations. Claerbout (1968) shows that the autocorrelation of a seismic response of a subsurface source recorded at the surface yields a reflection response as if both source and receiver are at the receiver location. Later it was derived from a seismic reciprocity theorem that an exact Green's function between two receiver locations in general inhomogeneous media can be retrieved from the crosscorrelations of wavefields from a closed boundary of sources surrounding the receiver locations (Wapenaar, 2004; van Manen et al., 2005). Other authors explain seismic interferometry using stationary phase theory (Schuster, 2001; Snieder, 2004) or physical arguments based on time reversal (Derode et al., 2003; Fink, 2006).

The VS theory (Wapenaar et al., 2005; Korneev and Bakulin, 2006) suggests that a correct response can be recovered by the VS method when both monopole and dipole sources are located on a closed surface surrounding the receivers. However, practical applications typically involve one-sided illumination with only limited surface aperture and single source types (Schuster and Zhou, 2006; Bakulin et al., 2007c). As this violates the original assumptions, artifacts can emerge and the amplitudes of VS data generally are distorted (Snieder et al., 2006). Wapenaar (2006) shows that the problem of one-sided illumination can be diminished by increasing the recording time, given sufficient scatterers exist below the receiver array. An important improvement of the VS method is suggested by Mehta et al. (2007), who reason that separation of the up- and downgoing wavefields before crosscorrelation would remove surface- and overburden-related multiples and provide responses as if the overburden between the sources and the receivers were homogeneous.

In this paper, we discuss the radiation characteristics of virtual sources in laterally invariant media in more detail. Our analysis is based on downhole receivers in a horizontal borehole, but it can be modified for different configurations such as receivers in deviated or vertical boreholes. We argue that even after wavefield separation, the retrieved VS data still inherit an imprint of the downgoing wavefields, caused by a finite aperture and the deployment of only a single source type at the earth's surface.

Our main geometry is depicted in Figure 1. Sources are located at depth level z_S, with source spacing Δx_S and the central source at $x_S = 0$. Receivers are located in a horizontal borehole at depth level z_R, with receiver spacing Δx_R and the central receiver at $x_R = 0$, right below the central source location. The medium above the receiver array is referred to as the overburden, generally having a strong het-
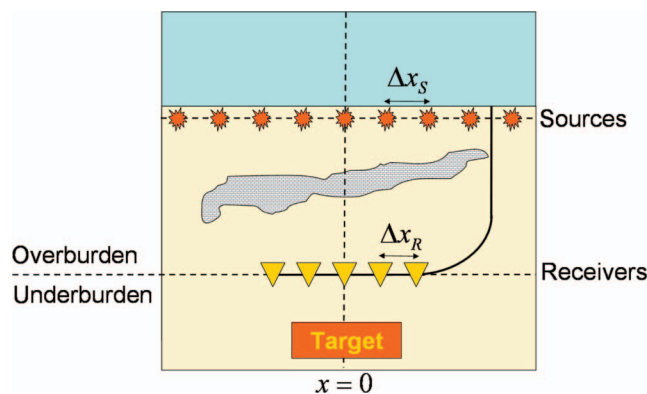

Figure 1. Configuration for the virtual source method. Downhole geophones are deployed in horizontal wells; sources are situated immediately under the earth's surface.

erogeneous character. The medium below the receiver array is the underburden. We seek to image the underburden without additional information about the overburden, the goal of the virtual source method.

First, we describe implementation of the VS method in the time-space or *t-x* domain. Then we place the virtual source in a laterally invariant medium and transform the equations to the frequency-wavenumber or *f-k* domain to show that the implemented methodology does not yield the desired reflection response. We separate the given equations in terms of amplitude and phase to show that the VS method provides an accurate phase response but may distort the amplitude response. This is explained in terms of the distortions in the amplitude radiation pattern of the virtual source. We show how this amplitude radiation pattern can be estimated in a laterally invariant medium and corrected for by deconvolution in the *f-k* domain. In addition, we show that time-gating the downgoing wavefield before crosscorrelation, a conventional processing step in implementation of the VS method, also contributes to a better amplitude radiation pattern. We demonstrate these concepts with a synthetic data set inspired by a field in Oman. Finally, we present some analog ideas for visualization of VS amplitude radiation characteristics in general inhomogeneous media and apply these to a synthetic data set based on a field from Canada.

THE VIRTUAL SOURCE METHOD IN THE TIME DOMAIN

Each shot that is fired results in a Green's function $G(x_R|x_S;t)$ between source location x_S (at depth z_S) and receiver location x_R (at depth z_R), convolved with the source wavelet $s(t)$. For simplicity, we omit the source wavelet and express our formulations as if all sources are impulsive. At this point, no assumptions on the source type have been made. For the receivers, we choose vertical geophones. We decompose the data, separate the up- and downgoing P-wavefields, and remove the S-waves, resulting in $G^+(x_R|x_S;t)$ and $G^-(x_R|x_S;t)$, representing the downgoing and upgoing P-wavefields, respectively, as registered by vertical geophones.

With the virtual source method, we want to retrieve the reflection response of the underburden by crosscorrelating the down- and upgoing wavefields and summing over the sources (Mehta et al., 2007). We refer to the response retrieved by this method as $R^{VS}(x_R|x'_R;t)$, where superscript VS stands for virtual source. The VS method can be interpreted as a discrete implementation of the following integral:

$$R^{VS}(x_R|x'_R;t) = \int G^+(x'_R|x_S;t) \otimes G^-(x_R|x_S;t)dx_S, \quad (1)$$

where $\otimes$ denotes temporal crosscorrelation and the integral takes place over the source coordinate x_S.

Strictly speaking, to retrieve an exact Green's function between two receivers in an elastic medium, theory suggests that both force and deformation sources are required on a closed boundary, surrounding the receivers, where the responses of deformation sources at one location need to be crosscorrelated with responses of force sources at the other location (Wapenaar and Fokkema, 2006). In the far-field high-frequency regime, this exact representation can be approximated by a single crosscorrelation of the particle velocity components, summed over source types equally distributed over a closed boundary. To arrive at equation 1 from this theory, we must incorporate the far-field high-frequency approximation, neglect the source

terms from below the receiver array, replace the multicomponent sources by single-component sources, and introduce wavefield separation, as suggested by Mehta et al. (2007).

The reflection response of the underburden also can be obtained by direct modeling. We refer to this response as $R^{\text{REF}}(x_R|x'_R;t)$, where superscript REF stands for reference. We can formulate the following forward equation to relate the upgoing wavefield at x_R to the downgoing wavefield at x'_R:

$$G^-(x_R|x_S;t) = \int R^{\text{REF}}(x_R|x'_R;t) \times G^+(x'_R|x_S;t)dx'_R, \qquad (2)$$

where $\times$ denotes temporal convolution. The integral takes place over receiver coordinate x'_R, where we assume the receiver array to be sufficiently sampled and extended as to capture the entire wavefield. Note that equation 2 has its major integral over the receivers, whereas equation 1 has its integral over the sources. Next, we show that if both equations are evaluated in a laterally invariant medium, they can be related to each other effectively in the f-k domain.

THE VIRTUAL SOURCE IN A LATERALLY INVARIANT MEDIUM

If the virtual source is placed in a medium without lateral variations, we can synthesize each source-receiver combination from the central shot record by spatial shifting. In this way, equation 1 can be rewritten as

$$R^{\text{VS}}(x_R - x'_R|0;t) = \int G^+(x'_R - x_S|0;t)$$
$$\otimes G^-(x_R - x_S|0;t)dx_S. \qquad (3)$$

We can now apply temporal Fourier transformation, followed by spatial Fourier transformation, over the receiver location x_R. We use the spatial Fourier transform shift theorem to arrive at

$$\widetilde{R}^{\text{VS}} \exp(ikx'_R) = \left\{ \int \hat{G}^+(x'_R - x_S|0;\omega) \right.$$
$$\left. \times \exp(-ikx_S)dx_S \right\}^* \widetilde{G}^-. \qquad (4)$$

Here, $\widetilde{G}^-$ represents the f-k representation of the upgoing wavefield of the central shot record $G^-(x_R|0;t)$ and $\widetilde{R}^{\text{VS}}$ is the f-k representation of $R^{\text{VS}}(x_R|0;t)$. The value $\hat{G}^+(x'_R - x_S|0;\omega)$ is a representation of $G^+(x'_R - x_S|0;t)$ in the frequency-space or f-x domain, where ω is the angular frequency. The term $\int \hat{G}^+(x'_R - x_S|0;\omega)\exp(-ikx_S)dx_S$ can be recognized as the spatial Fourier transform of $\hat{G}^+(-x_S|0;\omega)$ (written as $\widetilde{G}^+$), shifted over x'_R. We use the spatial Fourier transform shift theorem to rewrite equation 4 as

$$\widetilde{R}^{\text{VS}} \exp(ikx'_R) = \{\widetilde{G}^+\}^* \widetilde{G}^- \exp(ikx'_R) \qquad (5)$$

or

$$\widetilde{R}^{\text{VS}} = \{\widetilde{G}^+\}^* \widetilde{G}^-. \qquad (6)$$

The VS data in a laterally invariant medium thus can be represented by a multiplication of the complex conjugated downgoing field and the upgoing field of the central shot record in the f-k domain, given that both sources and receivers are sampled regularly. Here it is important that the receiver array is extended sufficiently to capture a fair representation of the wavefield. The receiver spacing needs to be small to avoid spatial aliasing in the f-k domain. Similarly, equation 2 can be rewritten in the f-k domain as (Kennett, 1983)

$$\widetilde{R}^{\text{REF}} = \frac{\widetilde{G}^-}{\widetilde{G}^+}, \qquad (7)$$

where $\widetilde{R}^{\text{REF}}$ is the f-k transform of the reference reflection response at the central receiver location $R^{\text{REF}}(x_R|x'_R = 0;t)$. Note that the virtual source is generated by means of a crosscorrelation of the down- and upgoing wavefields (equation 6), whereas the reference reflection response is a spatial deconvolution of these fields (equation 7). In the following section, we show that the phase spectrum of the reflection response is perfectly retrieved by the VS method but the amplitude spectrum is not.

AMPLITUDE AND PHASE

We can write the f-k representations of the data in terms of amplitude and phase according to $\widetilde{G}^\pm = |\widetilde{G}^\pm|\exp(i\widetilde{\phi}^\pm)$ and $\widetilde{R}^{\text{VS}} = |\widetilde{R}^{\text{VS}}|\exp(i\widetilde{\phi}^{\text{VS}})$. Substituting these representations into equation 6 yields, in terms of phase,

$$\widetilde{\phi}^{\text{VS}} = \widetilde{\phi}^- - \widetilde{\phi}^+. \qquad (8)$$

In terms of amplitude, it is

$$|\widetilde{R}^{\text{VS}}| = |\widetilde{G}^+||\widetilde{G}^-|. \qquad (9)$$

By writing the reference response as $\widetilde{R}^{\text{REF}} = |\widetilde{R}^{\text{REF}}|\exp(i\widetilde{\phi}^{\text{REF}})$, we can also rewrite equation 7 in terms of phase

$$\widetilde{\phi}^{\text{REF}} = \widetilde{\phi}^- - \widetilde{\phi}^+, \qquad (10)$$

and in terms of amplitude

$$|\widetilde{R}^{\text{REF}}| = \frac{|\widetilde{G}^-|}{|\widetilde{G}^+|}. \qquad (11)$$

Comparing equations 8 and 10, we observe that the VS method yields accurate predictions of the phase of the reference response. However, in terms of amplitudes, we find a different spectrum (compare equations 9 and 11). This is caused by the imperfect geometry having one-sided illumination and the use of a single source type at the earth's surface. Thus, it can be shown that the VS data and the reference response are related as

$$\widetilde{R}^{\text{VS}} = |\widetilde{G}^+|^2 \widetilde{R}^{\text{REF}}, \qquad (12)$$

where $|\widetilde{G}^+|^2$ can be interpreted as the VS amplitude radiation pattern. It originates from the imperfect illumination at the receiver array $|\widetilde{G}^+|$, affecting both the down- and the upgoing wavefields that are used in the crosscorrelation process. An ideal VS would be fed by a wavefield with uniform spatial distribution $|\widetilde{G}^+| = 1$.

AMPLITUDE RADIATION CORRECTION

If $|\widetilde{G}^+| \neq 1$, we propose to improve the VS method in laterally invariant media by the following amplitude radiation correction:

$$\widetilde{R}_{\text{CORRECTED}}^{\text{VS}} = \frac{\widetilde{R}^{\text{VS}}}{|\widetilde{G}^+|^2}. \tag{13}$$

Stable implementation of equation 13 would require $|\widetilde{G}^+| \neq 0$ for each direction of VS radiation. By introducing a stabilization factor and a tapered muting filter that eliminates parts of the *f-k* spectrum where $|\widetilde{G}^+| \to 0$, we can implement the correction in practice. However, the results still may not be optimal if the illumination has a preferential orientation. Mateeva et al. (2007) suggest steering the VS accordingly into the direction of our interest. Here, we propose to assign a new downgoing amplitude radiation pattern $|\widetilde{A}^{\text{RADIATION}}|$ and formulate for the steered VS:

$$\widetilde{R}_{\text{STEERED}}^{\text{VS}} = |\widetilde{A}^{\text{RADIATION}}| \frac{\widetilde{R}^{\text{VS}}}{|\widetilde{G}^+|^2}. \tag{14}$$

The filter $|\widetilde{A}^{\text{RADIATION}}|$ can be designed to suppress parts of the VS radiation pattern that are recovered inaccurately by equation 14, to steer the VS in any particular direction of interest, or to manipulate the radiation characteristics of the VS in terms of emitted frequencies.

THE EFFECTS OF TIME-GATING

The practice of time-gating the downgoing wavefield before crosscorrelation has always been an integral part of the virtual source method (Bakulin and Calvert, 2004, 2006). In essence, the time gate determines which part of the wavefield will be time reversed (in the crosscorrelation of equation 1). For P-wave imaging, the time gates usually are applied around the first arrivals (Bakulin and Calvert, 2006; Bakulin et al., 2007c). For S-wave imaging, the gates are placed around directly arriving shear waves in the receiver gathers (Bakulin et al., 2007b). In practical cases with finite aperture, limiting the time-reversed wavefield to the strongest arrivals of a particular kind leads to better VS data than crosscorrelating the entire wavefield as suggested by theory. Even if wavefield separation is applied at the preprocessing stage, time-gating successfully reduces artifacts and improves the signal-to-noise ratio of VS data (Mehta et al., 2007). These improvements have been explained on a physically

Figure 2. Configuration of the laterally invariant elastic model from Oman.

intuitive level. Here, we offer a more rigorous explanation in terms of the VS radiation pattern.

We define $\widetilde{G}_{\text{GATING}}^+$ as the *f-k* transform of the time-gated downgoing wavefield. In a similar fashion as for the ungated fields, we can derive that the VS data retrieved from gated fields can be written as

$$\widetilde{R}_{\text{GATING}}^{\text{VS}} = \{\widetilde{G}_{\text{GATING}}^+\}^* \widetilde{G}^-. \tag{15}$$

Once more we write the data in terms of amplitude and phase according to $\widetilde{G}_{\text{GATING}}^+ = |\widetilde{G}_{\text{GATING}}^+|\exp(i\widetilde{\phi}_{\text{GATING}}^+)$ and $\widetilde{R}_{\text{GATING}}^{\text{VS}} = |\widetilde{R}_{\text{GATING}}^{\text{VS}}|\exp(i\widetilde{\phi}_{\text{GATING}}^{\text{VS}})$. Substituting these representations into equation 15 yields, in terms of phase

$$\widetilde{\phi}_{\text{GATING}}^{\text{VS}} = \widetilde{\phi}^- - \widetilde{\phi}_{\text{GATING}}^+. \tag{16}$$

In terms of amplitude, it yields

$$|\widetilde{R}_{\text{GATING}}^{\text{VS}}| = |\widetilde{G}_{\text{GATING}}^+||\widetilde{G}^-|. \tag{17}$$

If we substitute equation 17 into equation 11 we find that the amplitude spectrum of the VS data from gated fields relates to the amplitude spectrum of the reference response as

$$|\widetilde{R}_{\text{GATING}}^{\text{VS}}| = |\widetilde{G}_{\text{GATING}}^+||\widetilde{G}^+||\widetilde{R}^{\text{REF}}|. \tag{18}$$

In the upcoming example, we show that the effects of time-gating on the phase are relatively small, in other words, $\widetilde{\phi}_{\text{GATING}}^+ \approx \widetilde{\phi}^+$. By neglecting the phase effect of time-gating, the VS data from gated fields can be described as

$$\widetilde{R}_{\text{GATING}}^{\text{VS}} \approx |\widetilde{G}_{\text{GATING}}^+||\widetilde{G}^+|\widetilde{R}^{\text{REF}}. \tag{19}$$

The product $|\widetilde{G}_{\text{GATING}}^+||\widetilde{G}^+|$ can be interpreted as the VS amplitude radiation pattern. Because $|\widetilde{G}_{\text{GATING}}^+|$ contains only the direct wave, which generally is quite uniform in nature and relatively unaffected by the subtleties of late time scattering, time-gating often improves the radiation characteristics of a virtual source, as we demonstrate in the following example.

EXAMPLE FROM OMAN

We test our theory for laterally invariant media on an elastic model from a Shell field in Oman. We visualize the velocity model and geometry in Figure 2. In this model, 321 vertical force sources are situated at a depth of $z_S = 2$ m with a source spacing $\Delta x_S = 5$ m. The upper 200 m of the overburden consists of finely layered material with large acoustic contrasts. Below 200 m, we find a homogeneous layer in which 81 receivers are situated at $z_R = 250$ m with spacing $\Delta x_R = 5$ m. In the underburden, we find four strong reflectors, A-D.

The up- and downgoing P- and S-wavefields are separated with elastic decomposition. Our decomposition is exact; however, for practical applications a dual-sensor approximation technique may be available, requiring only the registration of vertical particle velocity and pressure (Mehta et al., 2007). The downgoing P-wavefield at the central VS location is crosscorrelated with the upgoing P-wavefield as recorded by the other receivers. The resulting cross-correllograms are stacked over the source locations, resulting in the estimated reflection response $R^{\text{VS}}(x_R|x_R' = 0; t)$, according to equation 1, where $x_R' = 0$ denotes the location of the VS, which is chosen in the center of the receiver array. We compare the result with the reference response, obtained by placing a vertical force source at the VS location in an equivalent medium with the overburden replaced
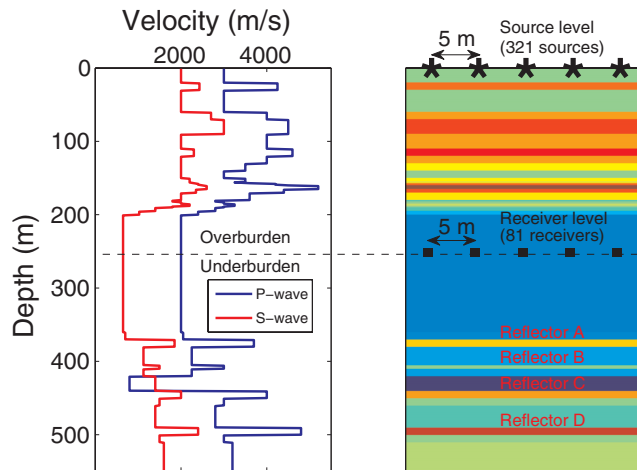
by a homogeneous half-space. The emitted S-waves are removed from the reference response by elastic decomposition. In Figure 3 we show the resulting VS data (in red) versus the reference response (in black). Although the VS data have a good kinematic match to the reference response, the amplitudes at larger offsets are not in agreement for the first two reflectors. Further, we observe improper convergence of the kinematics of some traces, for example at zero offset.

We now explain the differences of the directly modeled response and the retrieved VS data in terms of radiation characteristics in the *f-k* domain. First, we should mention that our directly modeled response is not exactly the assumed reference reflection produced by an explosive source. Instead, we modeled the response of a vertical force source to which the crosscorrelation-based VS method is supposed to converge (Mehta et al., 2007). This vertical force source has a clear radiation pattern that we can visualize by placing the source in a homogeneous medium and measuring the far-field excitation by a horizontal array of vertical geophones at depth and transforming the result to the *f-k* domain — see Figure 4. In Figure 5, we show the *f-k* transform of the directly modeled reference response, which we

interpret as the amplitude radiation pattern of the vertical force source (Figure 4) convolved with the actual response of the medium. In Figure 5 we can observe the imprint of the radiation pattern (Figure 4) superimposed on the imprint of the reflectors.

As derived, the radiation pattern of a virtual source in a laterally invariant medium can be described by the spatial autocorrelation of the downgoing wavefield $|\widetilde{G}^+|^2$, which we show in Figure 6. We can recognize the imprint of this pattern in the *f-k* transformed VS data, as shown in Figure 7. Above we derived how the radiation characteristics can be improved by amplitude radiation correction (equation 13). To optimize the comparison of radiation-corrected VS data (converging to the response of an explosive source) and the reference reflection response (computed with a vertical force source), we assign the radiation pattern of the vertical force source (Figure 4) to the corrected VS data. The *f-k* representation of the VS data after the radiation correction is shown in Figure 8. Note the improved convergence to the reference response (Figure 5). This is a clear indication that removing the radiation pattern can indeed improve the quality of VS data, but what does this mean in the time domain? In Figure 9, we show time-space representations of the reference response (in black)
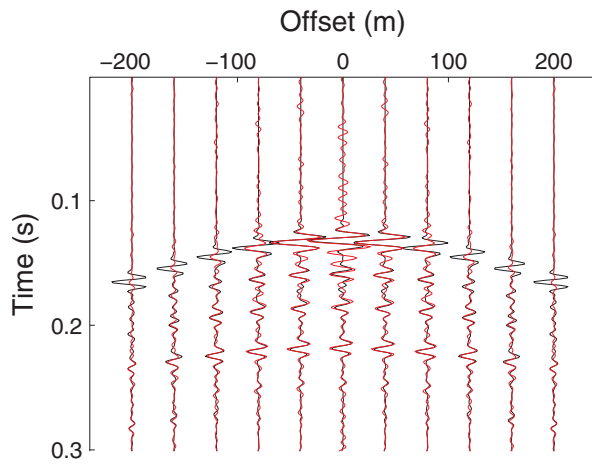

Figure 3. Shot record by a virtual source at the central receiver location generated by crosscorrelations of the total up- and downgoing wavefields (red) compared with the directly modeled reference response (black); vertical force sources are used at the earth's surface.

Figure 5. The *f-k* amplitude spectrum of the directly modeled reference reflection response; excited and recorded S-waves have been removed by elastic decomposition on the source and receiver side.
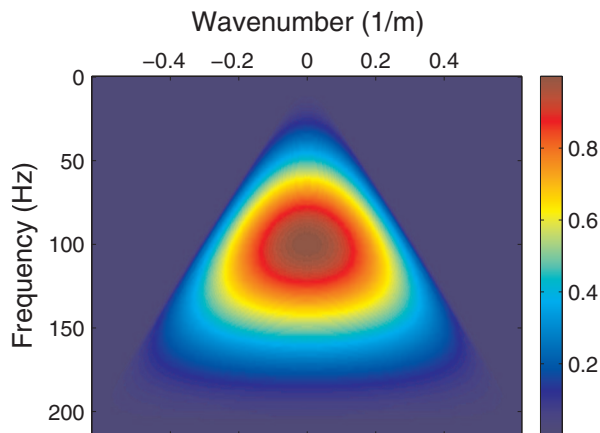

Figure 4. Far-field amplitude radiation pattern of a vertical force source, as observed by a horizontal array of vertical geophones at 250 m depth in a homogeneous medium with properties as in the receiver array of the model; excited S-waves have been removed.
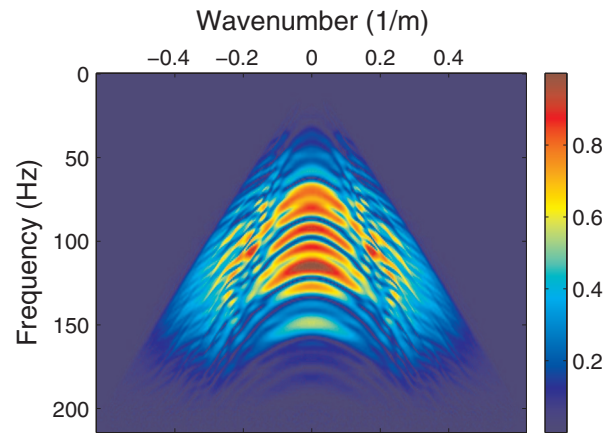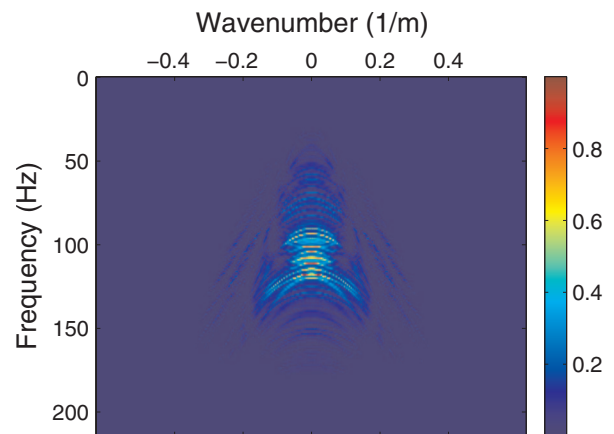

Figure 6. Estimated amplitude radiation pattern of a virtual source at the central receiver location generated from vertical force sources at the earth's surface.

and the corrected VS data (in red). The amplitude retrieval and kinematic match have improved, compared to the original data (Figure 3).

As we indicated, the type of sources fired at the surface can have a major impact on the quality of the retrieved VS data. To illustrate this, we repeat the experiments with horizontal instead of vertical force sources, still retrieving P-P reflections from vertical particle velocity recordings. In Figure 10, we show the time-domain representations of the retrieved VS data (in red), compared with the directly modeled reference response (in black). Because of the nonmatching characteristics of the illuminating downgoing wavefields and the desired radiation of the virtual source we aim to retrieve, we find a relatively poor match. This can be illustrated by the VS amplitude radiation pattern (Figure 11), being very different from the radiation pattern of the reference response (Figure 4). The *f-k* transformation of the VS data reveals a clear imprint of the VS radiation pattern (Figure 12). Applying amplitude radiation correction and assigning the desired radiation characteristics as they appear in the reference response (Figure 4), we can improve the *f-k* amplitude spectrum of the VS data drastically, as shown in Figure 13. Results

still are not perfect, as particular parts of the spectrum are not illuminated by the horizontal force sources and therefore cannot be retrieved (for example the data at zero horizontal wavenumber). We transform the VS data back to the time domain to illustrate that the convergence to the reference reflection response has improved (Figure 14). Despite the nonmatching radiation characteristics of the horizontal force sources at the earth's surface and the desired vertical force virtual source in the borehole, we can optimize the retrieved VS response by correcting the radiation characteristics of the generated virtual source.

Another and easier way to improve VS radiation characteristics that can be exported directly to general inhomogeneous media is time-gating. In Figure 15, we show VS data generated from vertical force sources with time-gating applied to the downgoing wavefields. Note the better kinematic match of VS data to the reference response compared to the results obtained from ungated data (Figure 3). To show that time-gating does not have a major impact on the phase of
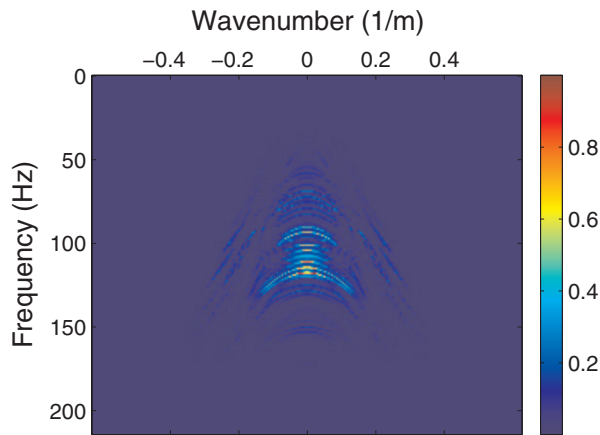

Figure 7. The *f-k* amplitude spectrum of a shot record by a virtual source at the central receiver location generated by crosscorrelations of the up- and downgoing wavefields; vertical force sources are used at the earth's surface.
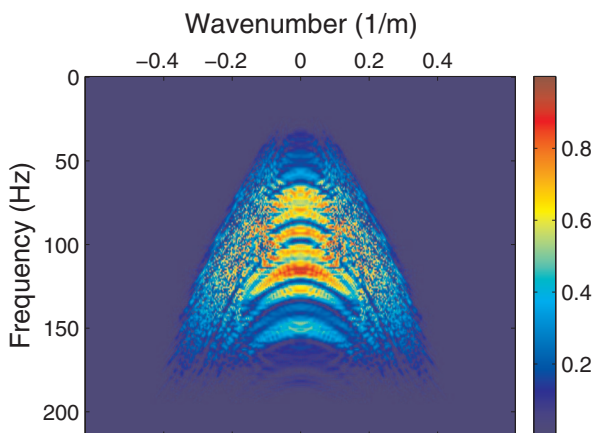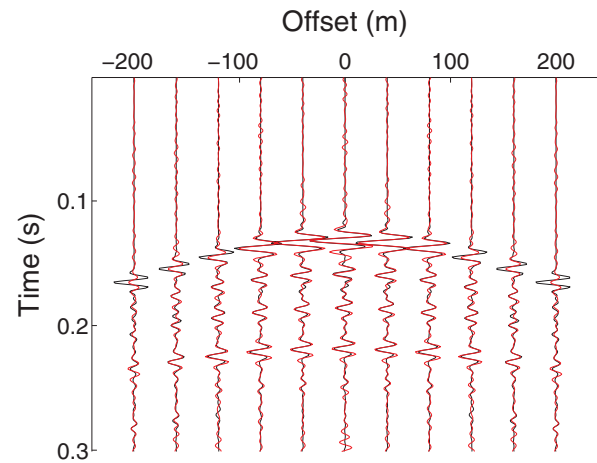

Figure 8. The *f-k* amplitude spectrum of a shot record by a virtual source at the central receiver location generated by crosscorrelations of the up- and downgoing wavefields after amplitude radiation correction; vertical force sources are used at the earth's surface.

Figure 9. Shot record by a virtual source at the central receiver location generated by crosscorrelations of the up- and downgoing wavefields after amplitude radiation correction (red) compared with the directly modeled reference response (black); vertical force sources are used at the earth's surface.
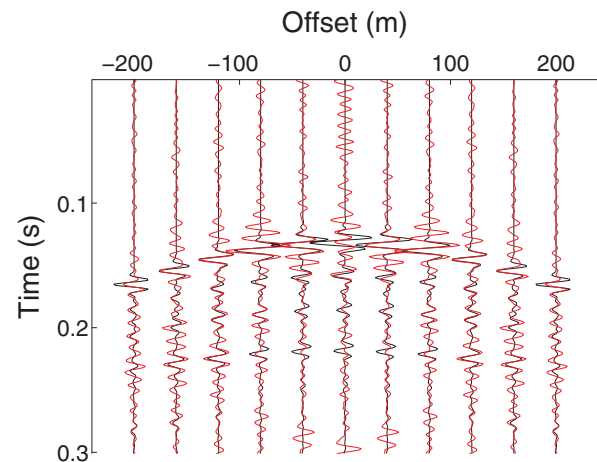

Figure 10. Shot record by a virtual source at the central receiver location generated by crosscorrelations of the up- and downgoing wavefields (red) compared with the directly modeled reference response (black); horizontal force sources are used at the earth's surface.

the signal, we computed the absolute phase difference between the gated and ungated downgoing wavefield of the central shot in Figure 16. For the relevant parts of the *f-k* spectrum that are illuminated, the phase difference is insignificant and the assumption $\widetilde{\phi}^+_{\text{GATING}} \approx \widetilde{\phi}^+$ is fulfilled. Therefore, we can estimate the VS radiation pattern as $|\widetilde{G}^+_{\text{GATING}}||\widetilde{G}^+|$, plotted in Figure 17. We obtain a more uniform radiation pattern by the time-gating step (compare with Figure 6), because the direct gated wavefield $|\widetilde{G}^+_{\text{GATING}}|$ is less affected by the characteristics of the medium of propagation, whereas later arrivals in $|\widetilde{G}^+|$ possess a strong imprint of medium-dependent scattering at later times. This is also reflected in the *f-k* amplitude spectrum of the generated VS data, which is shown (Figure 18), revealing a broader illumination than the results from ungated fields (Figure 7).

EXTENSION TO GENERAL INHOMOGENEOUS MEDIA

In general inhomogeneous media, equations 6 and 7 cannot be derived as such, and different techniques must be used for estimating

and correcting the VS radiation pattern. One possibility is to discretize equation 2 in the frequency domain, leading to a system of matrix equations that can be solved for the reflection response by least-squares inversion. This method has been proposed by various authors, either as Betti deconvolution (Holvik and Amundsen, 2005), least-squares redatuming (Schuster and Zhou, 2006), or multidimensional deconvolution (Wapenaar et al., 2008).

Alternatively, we could learn from our analysis that the local illumination of the downgoing wavefield at the virtual source location perturbs the VS radiation characteristics. In laterally invariant media, the illumination pattern is similar for all receivers and can be obtained directly from the downgoing wavefield of a single shot record. For laterally varying media, we may diagnose the illumination characteristics of the downgoing wavefield at a VS location by local Fourier transforms, such as spatially windowed *f-k* transforms, spatial wavelet transforms, or Wigner transforms. To illustrate these concepts, we focus on the use of Wigner transforms to unravel the illumination characteristics of the downgoing wavefield at a particu-
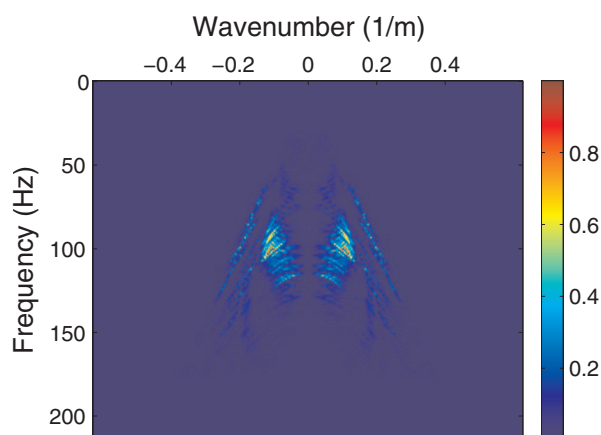

Figure 11. Estimated amplitude radiation pattern of a virtual source at the central receiver location generated from horizontal force sources at the earth's surface.
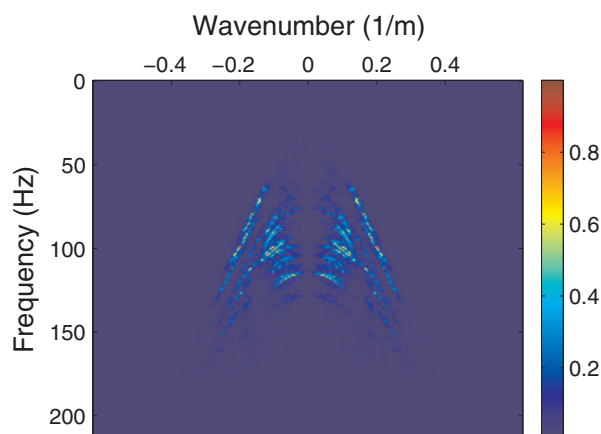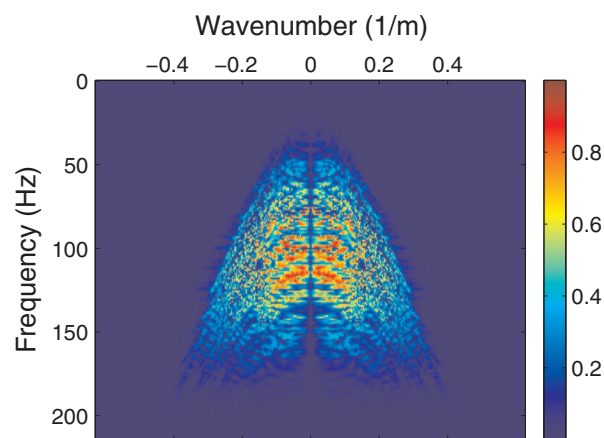

Figure 13. The *f-k* amplitude spectrum of a shot record by a virtual source at the central receiver location generated by crosscorrelations of the up- and downgoing wavefields after amplitude radiation correction; horizontal force sources are used at the earth's surface.

Figure 12. The *f-k* amplitude spectrum of a shot record by a virtual source at the central receiver location generated by crosscorrelations of the up- and downgoing wavefields; horizontal force sources are used at the earth's surface.
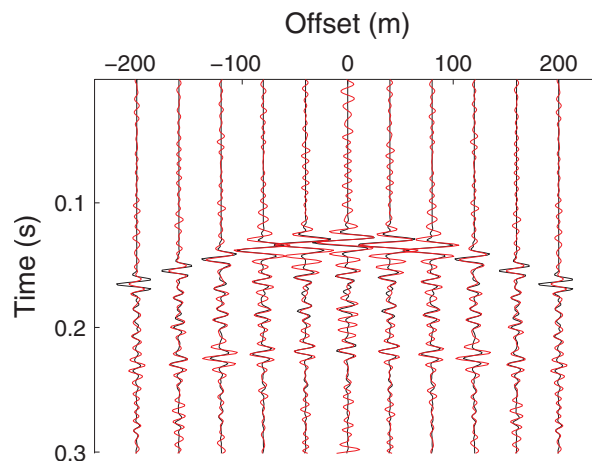

Figure 14. Shot record by a virtual source at the central receiver location generated by crosscorrelations of the up- and downgoing wavefields after amplitude radiation correction (red) compared with the directly modeled reference response (black); horizontal force sources are used at the earth's surface.

lar receiver location on a shot-to-shot basis. A Wigner transform $\widetilde{W}(x'_R, k, \omega)$ can be interpreted as a local Fourier transform at location x'_R, obtained through (Schleich, 2001)

$$
\widetilde{W}(x'_R, k, \omega) = \int_{-X}^{X} \left\{ \hat{G}^+\left(x'_R + \frac{1}{2}\zeta, \omega\right) \right\}^* \\
\times \hat{G}^+\left(x'_R - \frac{1}{2}\zeta, \omega\right) \exp(ik\zeta)d\zeta, \quad (20)
$$

where $\hat{G}^+(x'_R \pm \zeta/2, \omega)$ is the downgoing wavefield at location $x'_R \pm \zeta/2$ and superscript $*$ denotes complex conjugation. Equation 20 has much in common with the f-k transform, but instead of the full downgoing wavefield $\hat{G}^+(\zeta, \omega)$, we need two terms to sample each wavenumber, centered around the location of interest x'_R. Thus, we require twice as many sample points compared to an ordinary f-k transform to retrieve a single wavenumber. Therefore, the Wigner transform is twice as sensitive to spatial aliasing as the regular f-k transform. Ideally, the integral should take place over an infinite x-axis, but in practice, X as it occurs in equation 20 will be restricted to the geometry of the receiver array. The Wigner transform requires samples left and right of the receiver location x'_R, so it cannot be obtained at the edge of the array and resolution decreases with decreasing X. We will now illustrate the use of localized diagnostics with Wigner transforms using an example.

EXAMPLE FROM CANADA

We introduce a 2D synthetic example from Canada. A plot of the P-wave velocity model and sketch of the acquisition geometry is given in Figure 19. With spacing $\Delta x_S = 5$ m and depth $z_S = 15$ m, 321 explosive sources are placed under the earth's surface. The receiver array consists of 81 geophones with spacing $\Delta x_R = 10$ m at depth $z_R = 430$ m. Central receiver location 41 is located immediately under central source location 161. In the following analysis, source locations sA, sB, and sC correspond to source stations 121,
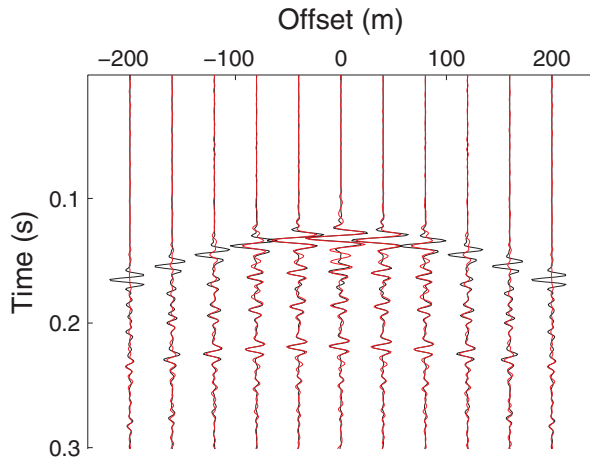

Figure 15. Shot record by a virtual source at the central receiver location generated by crosscorrelations of the total upgoing wavefield and the time-gated downgoing wavefield (red) compared with the directly modeled reference response (black); vertical force sources are used at the earth's surface.

Figure 17. Estimated amplitude radiation pattern of a virtual source at the central receiver location generated from vertical force sources at the earth's surface with time-gating applied to the downgoing wavefields.
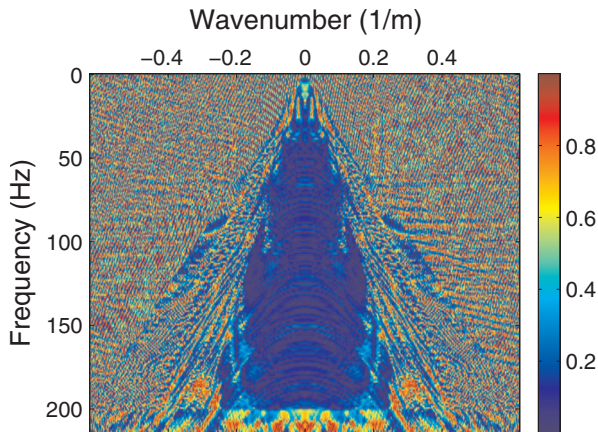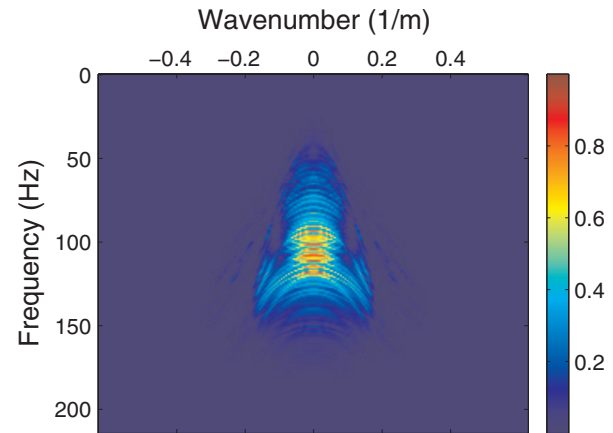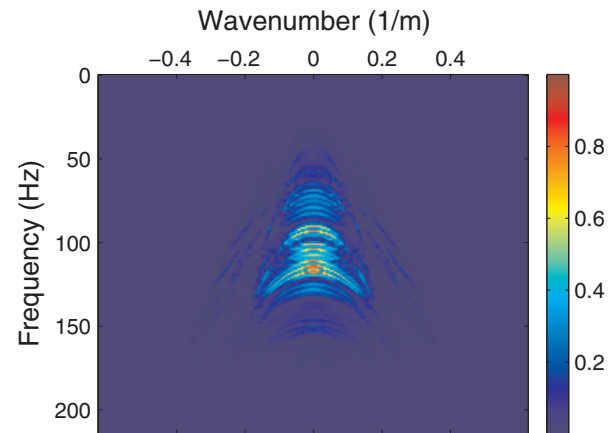

Figure 16. Absolute phase difference between the gated downgoing wavefield and the ungated downgoing wavefield of the central shot; blue colors are in phase; red colors are out of phase.

Figure 18. The f-k amplitude spectrum of a shot record by a virtual source at the central receiver location generated by crosscorrelations of the upgoing wavefields and the time-gated downgoing wavefields; vertical force sources are used at the earth's surface.

161, and 201, respectively, whereas receiver locations rA, rB, and rC correspond to receiver stations 21, 41, and 61, respectively. The upper 230 m of the subsurface is represented by a complex overburden with strong lateral and vertical variation in velocity. Below 230 m, the model consists of a simpler layered medium hosting the receiver array. Bakulin and Calvert (2006) show that robust results can be obtained by redatuming the shots to the downhole geophone locations by time-gating the downgoing wavefields at a virtual source location
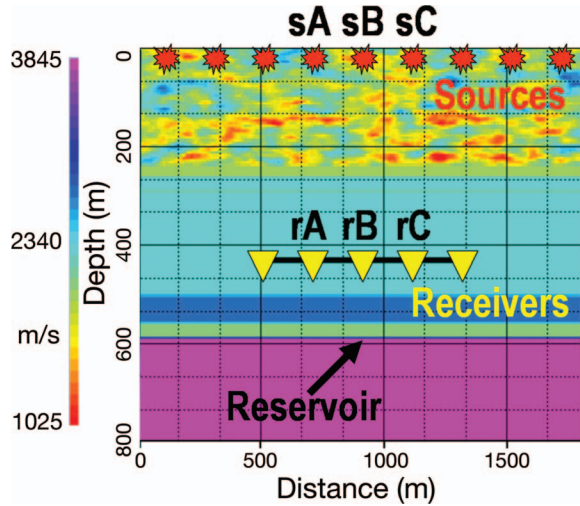

Figure 19. Configuration and P-wave velocities of the laterally variant example from Canada. The sources are at 5 m depth with 5 m spacing, and source stations ranging from 1 to 321. The receivers are at 430 m depth with 10 m spacing, and receiver stations ranging from 1 to 81. Source locations sA, sB, and sC denote source stations 121, 161, and 201, being located above receiver locations rA, rB, and rC, denoting receiver stations 21, 41, and 61.
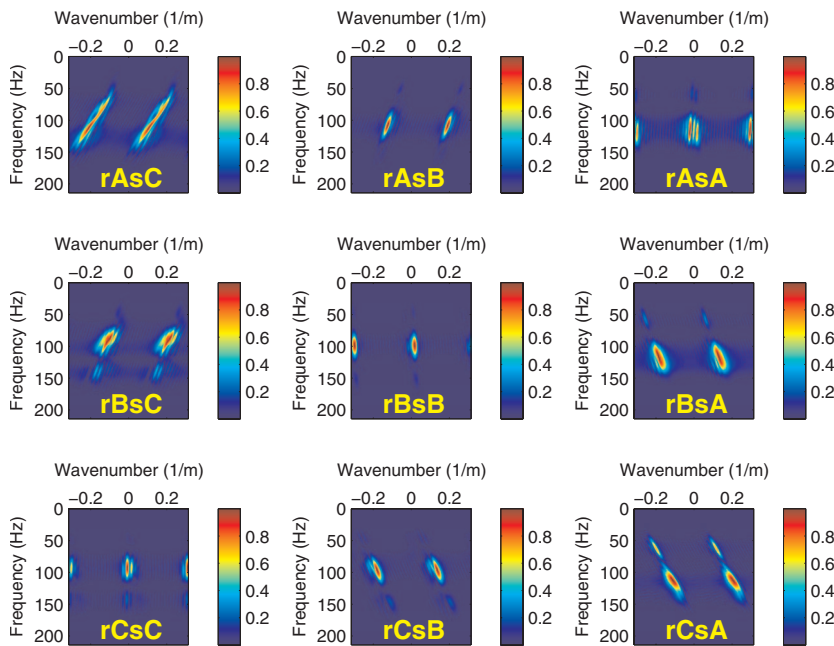
and crosscorrelating them with the total wavefields as registered elsewhere in the receiver array and stacking over the sources.

Here we show that the illumination characteristics at the virtual source location can be monitored effectively from shot to shot by using a Wigner transform, as described by equation 20. We select the receiver locations rA, rB, and rC and compute the Wigner transforms of the time-gated downgoing wavefields of three sources located at sA, sB, and sC (see Figure 19), where X is taken as 20 m. Results are shown in Figure 20. Note that the Wigner transform yields a local response of the wavefield of each shot at the depicted receiver location, providing information on the angle of propagation and frequency content. For a laterally invariant overburden this pattern is dependent only on the source-receiver offset, although for the general heterogeneous case this does not need to be true. For example, the illumination of source sC at receiver location rB has a different frequency content than the illumination of source sB at receiver location rA, whereas source-receiver offsets are identical in both cases. Therefore, a virtual source at rB will probably have different radiation characteristics than a virtual source at rA. With Wigner transforms (or other local f-k transforms), we can track the downgoing wavefield and obtain insight into the contribution of each shot to the VS radiation pattern. By summing the Wigner transforms of all shots at a fixed receiver, we might obtain a cumulative response that we could interpret as an estimate of the radiation pattern of a virtual source at this location. Radiation characteristics distorted by the overburden may then be improved by following a similar methodology as described for laterally invariant media or by simple source weighting before crosscorrelation. In addition, sources with undesired illumination can be excluded from the virtual source summation. In this way we obtain better control on designing radiation characteristics and steering of the virtual source.

DISCUSSION

This work may have an impact on VS seismics in horizontal wells and in particular on time-lapse monitoring with virtual sources. For instance, even in the case of a complex changing overburden and nonrepeatable surface acquisition, we might be able to manufacture virtual sources with identical radiation patterns. This could lead to repeatable time-lapse VS data free of amplitude distortions, which is the aim of virtual source monitoring from horizontal wells (Bakulin et al., 2007a). In addition, suggested diagnostics should improve passive imaging techniques substantially (Hohl and Mateeva, 2006; Draganov et al., 2007) by understanding passive noise illumination patterns and correcting for them. If passive noise sources are shown to have reasonable radiation patterns, then the described techniques may open ways to use them for time-lapse monitoring.

CONCLUSION

The amplitude radiation pattern of a virtual source in a laterally invariant medium can be estimated in the f-k domain by autocorrelation of the original downgoing wavefields. For these media,

Figure 20. Wigner transforms for various source locations sA, sB, and sC and receiver locations rA, rB, and rC. In addition to the real event, each panel shows at least one aliased event.

retrieved VS data can be improved by spatial deconvolution with the estimated amplitude radiation pattern. VS radiation characteristics depend strongly on the type of sources that are fired at the surface. We showed that the proposed radiation correction can drastically improve virtual sources generated by various source types, for example vertical force virtual sources generated from horizontal force sources at the earth's surface. Even though it is important to realize that we leave the phase of the signal untouched, the radiation correction improves the amplitudes and kinematics of VS data and can eliminate spurious events. Radiation correction applied to VS data generated from a laterally invariant elastic model from Oman significantly improved retrieved amplitudes and kinematics. It may be possible to extend the radiation correction concept to general inhomogeneous media by estimating the local radiation pattern of the VS or by replacing the proposed deconvolution step in the f-k domain by a multidimensional matrix inversion in the frequency domain, commonly known as Betti deconvolution, least-squares redatuming, or multidimensional deconvolution. Another way to improve VS radiation characteristics is to time-gate the direct arrival of the downgoing wavefield before crosscorrelating, as is already common practice in implementation of the VS method. Our evaluation in the f-k domain demonstrates the power of time-gating in improving the VS radiation pattern.

ACKNOWLEDGMENTS

REFERENCES

Bakulin, A., and R. Calvert, 2004, Virtual source: New method for imaging and 4D below complex overburden: 74th Annual International Meeting, SEG, Expanded Abstracts, 2477–2480.
——–, 2005, Virtual shear source: A new method for shear-wave seismic surveys: 75th Annual International Meeting, SEG, Expanded Abstracts, 2633–2636.
——–, 2006, The virtual source method: Theory and case study: Geophysics, **71**, no. 4, SI139–SI150.
Bakulin, A., J. Lopez, A. Mateeva, and I. Sinha Herhold, 2007a, Onshore monitoring with virtual-source seismic in horizontal wells: Challenges and solutions: 77th Annual International Meeting, SEG, Expanded Abstracts, 2893–2897.
Bakulin, A., A. Mateeva, R. Calvert, P. Jorgensen, and J. Lopez, 2007b, Virtual shear source makes shear waves with airguns: Geophysics, **72**, no. 2, A7–A11.
Bakulin, A., A. Mateeva, K. Mehta, P. Jorgensen, J. Ferrandis, I. Sinha Herhold, and J. Lopez, 2007c, Virtual source applications to imaging and reservoir monitoring: The Leading Edge, **26**, 732–740.
Campillo, M., and A. Paul, 2003, Long-range correlations in the diffuse seismic coda: Science, **299**, 547–549.
Claerbout, J. F., 1968, Synthesis of a layered medium from its acoustic transmission response: Geophysics, **33**, 264–269.
Derode, A., E. Larose, M. Tanter, J. de Rosny, A. Tourin, M. Campillo, and M. Fink, 2003, Recovering the Green's function from field-field correlations in an open scattering medium: Journal of the Acoustical Society of America, **113**, 2973–2976.
Draganov, D., K. Wapenaar, W. Mulder, J. Singer, and A. Verdel, 2007, Retrieval of reflections from seismic background-noise measurements: Geophysical Research Letters, **34**, L04305-1–L04305-4.
Fink, M., 2006, Time-reversal acoustics in complex environments: Geophysics, **71**, no. 4, SI151–SI164.
Hohl, D., and A. Mateeva, 2006, Passive seismic reflectivity imaging with ocean-bottom cable data: 76th Annual International Meeting, SEG, Expanded Abstracts, 1560–1564.
Holvik, E., and L. Amundsen, 2005, Elimination of the overburden response from multicomponent source and receiver seismic data, with source designature and decomposition into PP-, PS-, SP-, and SS-wave responses: Geophysics, **70**, no. 2, S43–S59.
Hornby, B. E., J. Yu, J. A. Sharp, A. Ray, Y. Quist, and C. Regone, 2006, VSP: Beyond time-to-depth: The Leading Edge, **25**, 446–452.
Kennett, B. L. N., 1983, Seismic wave propagation in stratified media: Cambridge University Press.
Korneev, V., and A. Bakulin, 2006, On the fundamentals of the virtual source method: Geophysics, **71**, no. 3, A13–A17.
Mateeva, A., A. Bakulin, P. Jorgensen, and J. Lopez, 2006, Accurate estimation of subsalt velocities using virtual checkshots: Offshore Technology Conference, OTC 17869.
Mateeva, A., J. Ferrandis, A. Bakulin, P. Jorgensen, C. Gentry, and J. Lopez, 2007, Steering virtual sources for salt and subsalt imaging: 77th Annual International Meeting, SEG, Expanded Abstracts, 3044–3048.
Mehta, K., A. Bakulin, J. Sheiman, R. Calvert, and R. Snieder, 2007, Improving the virtual source method by wavefield separation: Geophysics, **72**, no. 4, V79–V86.
Schleich, W. P., 2001, Quantum optics in phase space: Wiley-VCH.
Schuster, G. T., 2001, Theory of daylight / interferometric imaging: Tutorial: 63rd Annual International Conference and Exhibition, EAGE, Extended Abstracts, A32.
Schuster, G. T., and M. Zhou, 2006, A theoretical overview of model-based and correlation-based redatuming methods: Geophysics, **71**, no. 4, SI103–SI110.
Snieder, R., 2004, Extracting the Green's function from the correlation of coda waves: A derivation based on stationary phase: Physical Review E, **69**, 046610-1–046610-8.
Snieder, R., K. Wapenaar, and K. Larner, 2006, Spurious multiples in seismic interferometry of primaries: Geophysics, **71**, no. 4, SI111–SI124.
van Manen, D.-J, J. O. A. Robertsson, and A. Curtis, 2005, Modeling of wave propagation in inhomogeneous media: Physical Review Letters, **94**, 164301-1–164301-4.
Wapenaar, K., 2004, Retrieving the elastodynamic Green's function of an arbitrary inhomogeneous medium by cross correlation: Physical Review Letters, **93**, 254301-1–254301-4.
Wapenaar, K., 2006, Green's function retrieval by crosscorrelation in case of one-sided illumination: Geophysical Research Letters, **33**, L19304-1–L19304-6.
Wapenaar, K., and J. Fokkema, 2006, Green's function representations for seismic interferometry: Geophysics, **71**, no. 4, SI33–SI46.
Wapenaar, K., J. Fokkema, and R. Snieder, 2005, Retrieving the Green's function in an open system by crosscorrelation: A comparison of approaches: Journal of the Acoustical Society of America, **118**, 2783–2786.
Wapenaar, K., E. Slob, and R. Snieder, 2008, Seismic and electromagnetic controlled-source interferometry in dissipative media: Geophysical Prospecting, **56**, 419–434.
Weaver, R. L., and O. I. Lobkis, 2002, On the emergence of the Green's function in the correlations of a diffuse field: Pulse-echo using thermal phonons: Ultrasonics, **40**, 435–439.
Willis, M. E., R. Lu, X. Campman, M. N. Toksöz, Y. Zhang, and M. V. de Hoop, 2006, A novel application of time-reversed acoustics: Salt-dome flank imaging using walkaway VSP surveys: Geophysics, **71**, no. 2, A7–A111.